Heliyon 8 (2022) e10258

Contents lists available at ScienceDirect

Heliyon

journal homepage: www.cell.com/heliyon

Research article

# Chitosan/carboxymethyl cellulose wound dressings supplemented with biologically synthesized silver nanoparticles from the ligninolytic fungus Anamorphous *Bjerkandera* sp. R1

Jerónimo Osorio Echavarría [a,*], Natalia Andrea Gómez Vanegas [a], Claudia Patricia Ossa Orozco [b]

[a] *Bioprocess Group, Department of Chemical Engineering, University of Antioquia, Street 70 # 52 – 21, Medellin 1226, Colombia*
[b] *Biomaterials Research Group, Bioengineering Program, University of Antioquia, Street 70 # 52 – 21, Medellin 1226, Colombia*

ARTICLE INFO

*Keywords:*
Biosynthesis
Biocompatibility
Chitosan (CHI)
Carboxymethyl Cellulose (CMC)
Silver Nanoparticles (AgNPs)
Anamorphous *Bjerkandera* sp. R1
Wound Dressing
Nanomaterial
Synthesis by fungi

ABSTRACT

Chitosan (CHI) and carboxymethyl cellulose (CMC) are naturally sourced materials with excellent physical, chemical, and biological properties, which make them a promising tool for the development of different medical devices. In this research, CHI-CMC wound dressings were manufactured, by using different colloidal suspensions of silver nanoparticles (AgNPs) synthesized from the ligninolytic fungus Anamorphous *Bjerkandera* sp. R1, called CS and SN. Transmission electron microscopy (TEM), UV-Vis spectroscopy, and dynamic light scattering (DLS) analysis were used to characterize AgNPs. The wound dressings were characterized, by scanning electron microscopy (SEM), optical microscopy and their mechanical, antimicrobial, and biological properties were evaluated. The results of the different characterizations revealed the formation of spherical AgNPs with a mean size between 10 and 70 nm for the different mixtures worked. The mechanical properties of CHI-CMS-AgNPs doped with CS and SN suspensions showed superior mechanical properties with respect to CHI-CMC wound dressings. Compared to the latter, CHI-CMC-AgNPs wound dressings yielded better antibacterial activity against the pathogen *Escherichia coli*. In biological assays, it was observed that manufactured CHI-CMC-AgNPs wound dressings were not toxic when in contact with human skin fibroblasts (Detroit). This study, then, suggests that this type of wound dressings with a chitosan matrix and carboxymethyl cellulose doped with biologically synthesized nanoparticles from the fungus *Bjerkandera* sp., may be an ideal alternative for the manufacture of new wound dressings.

## 1. Introduction

Human skin is the first and main barrier against the invasion of external agents, which are harmful to the body. It represents approximately 15% of an adult's total body weight and has an area of 1.5–2 $m^2$, by making it the largest organ in the human body [1, 2]. According to the Wound Healing Society, skin wounds occur when cellular integrity is compromised due to mechanical, physical, or metabolism-related problems [3]. These wounds can be divided, from a clinical point of view, into acute and chronic wounds. Regarding acute wounds, the injury can be caused by a variety of factors, by including radiation, extreme temperature changes, or contact with chemicals. This type of wound can heal spontaneously in 8–12 weeks. On the other hand, chronic wounds usually require a longer healing time (months), due to intrinsic factors related to inflammation. They can occur from a number of causes, by including tumors, infections, or physical agents [4].

For the treatment of such wounds, it is essential to ensure different coordinated processes involving mainly various resident and migratory cells and components of the extracellular matrix (EMC), as well as an appropriate healing time, which depends on the size and number of skin layers which have been affected [3]. Because most of these wounds are often accompanied by inflammations, which lead to bacterial infections generated by reactive oxygen species (ROS) [4], treatment is difficult and high costs are generated in medical procedures. Alternatively, the use of dressings of biocompatible materials supplemented with antimicrobial agents has arisen, which protect the wound from external pathogens and that can guarantee an optimal healing process [5, 6].

A dressing is described as a product capable of creating a wound-healing environment, designed in order to absorb exudate, to provide

* Corresponding author.
*E-mail address:* jeronimo.osorio@udea.edu.co (J. Osorio Echavarría).

https://doi.org/10.1016/j.heliyon.2022.e10258
Received 8 May 2021; Received in revised form 8 November 2021; Accepted 2 August 2022
2405-8440/© 2022 Published by Elsevier Ltd. This is an open access article under the CC BY-NC-ND license (http://creativecommons.org/licenses/by-nc-nd/4.0/).

an optimal balance of moisture on the wound surface, to prevent maceration of surrounding tissues, and to control bacterial colonization. Its main objective is to preserve the basic biological principles of moisture, heat, oxygenation, and blood circulation [7]. Among the most used biomaterials for its manufacture are natural polymers. Some of them, homoglycans, such as chitin and chitosan (CS) structured in nanofibers and scaffold-based cellulose; heteroglycans, such as alginates and carrageenan-based hydrogels and proteins, such as collagen and keratin-based sponges, have been widely used in the field of regenerative medicine, due to their biodegradability and high biocompatibility [8, 9].

Among the most commonly used natural polymers for dressings, chitosan, a poly-N-acetyl-glycosaminoglycan usually obtained by alkaline deacetylation of chitin [8, 10, 11], has attracted considerable attention for dressing development due to its broad antimicrobial spectrum and that it can promote wound healing, by activating fibroblasts, by regulating deposition of collagen fibers, and by facilitating cell migration [11, 12, 13, 14, 15]. On the other hand, carboxymethylcellulose (CMC), is a natural polyelectrolyte derived from cellulose, by containing a carboxymethyl group (–CH2COOH) [16], and it has also played an important role in biomedical applications [17] because it has a high water-binding capacity, good compatibility with the skin and mucous membrane. It has been used as a single material or combining it with drugs, in bandages for wound treatment [17, 18].

Over the past few decades, it has been reported that silver nanoparticles (AgNPs) exhibit remarkably unusual physical-chemical properties and elevated biological activities, for which they have been, for example, widely used in regenerative medicine for the manufacture of scaffolds in tissue engineering [19, 20]. These nanostructures have become very important due to their broad antimicrobial spectrum against various strains of bacteria, including Salmonella, Staphylococcus, Pseudomonas, among others [21]. In order to increase the use of AgNPs in regenerative medicine, it is important to consider some physicochemical properties, which include size (surface area), shape, surface load and coating, agglomeration, and dissolution rate because they are particularly important for determining their biological interactions and impacts [22, 23]. In this regard, efforts have been made to implement new AgNPs synthesis processes, which improve these properties, within existing methods. The use of biological methods can be considered an interesting tool as it is a non-toxic method because it does not require hazardous materials on the surface of nanomaterials, as well as being inexpensive and environmentally friendly [24]. Among the organisms involved in the biological synthesis of AgNPs, the implementation of fungi is proposed as an excellent route of synthesis because these microorganisms can over express specific reducing molecules and biocompatible coating agents, which facilitate the control of the size and shape of synthesized nanoparticles [24].

Considering the incorporation of AgNPs as a coating in medical products can, therefore, be a promising tool for future in vivo dressing applications. It is believed that combining these with biologically synthesized AgNPs by fungi can be highly beneficial in the wound healing process since the combination could act on wounds in two ways. First, the cell growth-promoting action of proteins found in biopolymers, such as chitosan and carboxymethyl cellulose, and second, the broad-spectrum antimicrobial action of AgNPs on wound-affecting microbes, as well as the low toxicity they can offer [10, 25, 26, 27, 28]. The objective of this research was to manufacture and to evaluate films based on chitosan and carboxymethyl cellulose supplemented with biologically synthesized AgNPs in order to determine their physical-mechanical properties and possible use as a wound dressing.

## 2. Methodology

### 2.1. Biosynthesis and characterization of silver nanoparticles (AgNPs) from fungus Anamorphous Bjerkandera sp. R1

Ligninolytic fungus strain Bjerkandera sp. R1 was donated by the Group of Environmental Biotechnology from the department of chemical engineering at Universidad de Santiago de Compostela (Spain) [29]. The reagents necessary for the preparation of the culture media and the synthesis of silver nanoparticles were donated by the bioprocess group from the department of chemical engineering at Universidad de Antioquia (Colombia). Regarding silver nanoparticle biosynthesis (AgNPs), ligninolytic fungus Anamorphous *Bjerkandera* sp. R1 was used. The growth of the fungus was carried out for an 8-day period, in 100 mL flasks with 40 mL of Modified Kirk's medium at pH 5.5 [30, 31, 32]. These were incubated at 30 °C with 175 rpm shaking stirring. In terms of synthesis, two methods were evaluated: (1) bio-reduction of silver ions in the crop supernatant (CS colloidal suspension) and (2) bio-reduction of silver ions from mycelium-pellet sediment (SN colloidal suspension). In both cases, pellets (fungal material) were washed with deionized water, and both the washed sediments (1% w/v) and the fungal extract obtained (1% v/v) from the growth process (8 days) were treated with a separate silver nitrate solution ($AgNO_3$). An initial concentration of this solution was assessed 1 mM. Both samples were adjusted to a pH 9.0 and incubated (T: 35 °C) in the dark at 175 rpm by 144 h, all growing conditions and subsequent synthesis were selected from previous studies [31, 33].

UV-Vis spectroscopy was performed to corroborate the formation of silver nanoparticles, by measuring the absorbance of SN and CS samples, by making 300–800 nm spectrophotometric scans on synergy H1 spectrofluorometer, biotech. To evaluate the size of the AgNPs was performed by Transmission Electron Microscope (TEM-JEOL-JSM 6490 LV) with an accelerating voltage of 20 kV; and finally, Micrometrics Nanoplus-3 Dynamic Light Scattering was used to observe the size and distribution of synthesized AgNPs (Tecnai F20 Super Twin TMP) and Dynamic Light Scattering (Micrometrics Nanoplus-3 Dynamic Light Scattering) analysis.

### 2.2. Dressings with the addition of silver nanoparticles

For the preparation of the chitosan (Sigma-Aldrich) (CHI) and carboxymethyl cellulose (Chemi S.A.S) (CMC) dressings, the steps were as follows: In the first instance, the CHI solution was prepared, by dissolving chitosan powder into an aqueous solution of 2 % glacial acetic acid (v/v). Then, mixed the CMC solution (1.2% w/w (dry base of CHI weight)) and stirred vigorously for 2 h. The dispersion of AgNPs (CS and SN colloidal suspensions) was diluted in the CHI-CMC solution at a ratio of 1% v/v and mixed for another 15 min. Finally, for the plasticization process, glycerol was added at 30% w/w on the dry basis of CHI weight, stirring it for 3 min. Once the wound dressings forming solutions were prepared, 20 mL of each solution was placed in glass molds (70 × 70 mm and 3 mm deep) and then, dried at 25 °C for 72 h [34]. All conditions for the preparation of wound dressings were selected from previous studies.

### 2.3. Characterization of chitosan/carboxymethyl cellulose-AgNPs dressings

CHI/CMC/AgNPs wound dressings were characterized, by using scanning electron microscopy (SEM) (JEOL JSM-6490LV) and optical microscopy in order to evaluate material surface and surface morphology before and after the addition of silver nanoparticles (AgNPs).

### 2.4. Antimicrobial assays

The antimicrobial activity of CHI/CMC/AgNPs composite dressings was determined, by using *Escherichia coli* [35, 36]. For reactivation, the strain was grown in 5 ml of nutritious broth for 24 h. Then, 100 μL of bacterial broth were grown Petri dishes in bacteriological agar. The agar diffusion method was used and the solutions that were prepared to manufactured the wound dressings containing AgNPs was submerged in 0.2 mm filter paper (diameter 12 mm) for the different tests. The plates were incubated at 37 °C for 24 h. After incubation, the inhibition zone around the filter paper [28, 31], was measured. Statistical validation was performed in this experiment in order to confirm whether there was a statistically significant difference over the inhibition halo.

### 2.5. Mechanical assays

The mechanical properties of the wound dressings were determined, by using a DBBP-20 universal machine (Bongshin, Korea) in accordance with the standardized method in ASTM D882-91 (ASTM, 2001). In order to determine maximum tensile strength (TS, MPa), elasticity module (EM, MPa), and maximum elongation (EB, %), the wound dressings were cut into rectangular parts (65 mm × 12 mm) and fastened from machine jaws. Statistical validation was performed in this experiment to confirm whether there was a statistically significant difference in tensile strength.

### 2.6. Cell viability assay

Indirect toxicity of wound dressings on Detroit cells (Human Skin Fibroblasts) was determined, by applying the method that uses the mitochondrial enzyme succinate-dehydrogenase (MTT). The materials were incubated in DMEM (basal medium) with bovine fetal serum (SFB) at 10% for 24 h at 37 °C. In parallel, Detroit cells were grown in plates of 96 wells for 24 h. Concentrations from 100% (undiluted) to 3.12% were evaluated. Dimethyl sulfoxide (DMSO) was incubated for 72 h at 37 °C, 5 % carbon dioxide (CO2). this reagent was used as a positive toxicity control at 6%. After incubation, both MTT and DMSO was added and the absorbance was determined at 570 nm in a spectrophotometer. The feasibility percentage of cells cultured with the extract of the materials was established. The assays were conducted in two independent experiments and with two replicates per assay.

## 3. Results and discussion

### 3.1. Characterization of silver nanoparticles synthesized from the ligninolytic fungus *Anamorphous* Bjerkandera *sp. R1*

In the first instance, a standardization process was performed in order to observe the physicochemical characteristics of biologically synthesized silver nanoparticles (AgNPs). Figure 1 shows a prominent surface plasmon resonance absorption (SPR) peak, centered at 400 nm for the CS colloidal suspension and 425 nm for the SN colloidal suspension. These results correspond to the formation of AgNPs [36, 37, 38]. The SPR is the most important optical property of this type nanostructures. This physical phenomenon consists of a collective oscillation of the conduction electrons in a metal, when the electrons are moved away from their equilibrium positions, in this case, by an electromagnetic wave (light). When the frequency of the light wave and the intrinsic frequency of the collective electron oscillations in Ag NPs coincide, an increase in scattering resonance and light absorption occurs [39, 40]. Regarding this, previous studies have shown that the intensity and shape of the absorption band (SPR) can give insight into different properties of AgNPs, including size, dielectric constants, shape, the amount synthesized in solution and the interaction between them [40, 41, 42, 43] By considering that within the SN suspension there was a rightward shift (red offset) at the maximum wavelength at the SPR peak (425 nm) (Figure 1b) with respect to the CS suspension (400 nm) (Figure 1a), and significantly decreased the absorbance, it can possibly be inferred that within the SN sample, the size of AgNPs increased and there was a lower concentration of them within the suspension [39, 44, 45]. The decrease in absorption peak intensity is caused by a decrease in the concentration of Ag NPs. This concentration decreases due a strong conglomeration of Ag NPs into larger particles. besides, the 25-nm shift can be explained possibly by an increase in the size of Ag NPs and it also caused by this factor. In this case, the nucleation and growth processes of silver nanoparticles could be affected by this type of synthesis.

Moreover, TEM analyses were performed in order to determine the morphology and size of synthesized AgNPs. In TEM micrographs (Figure 2), quasi-spherical particles can be observed in a range between 10 and 60 nm, for different colloidal suspensions. By means of an EDS analysis, coupled to the TEM, an optical absorption peak of approximately 3 keV was observed, which is typical for the absorption of silver nanocrystals [46] (Figure 2). The spectrum also yielded peaks in oxygen and carbon. These peaks possibly showed protein residues, which performed the stabilization function of AgNPs (Figure 2) [37, 47]. As for Dynamic Light Scatter Analysis (DLS), Figure 2e and 2f show the complete characterization of the AgNPs' size frequency based on the number of particles. It can be observed that smaller particles are predominant working in these conditions. For this experiment, a range of AgNPs sizes synthesized between 10 and 65 nm was obtained for both suspensions. With respect to the CS colloidal suspension, the smallest sizes were found, with close values comprising 10 and 50 nm. The scatter index (SI) value of silver nanoparticles was on average 0.25 for both samples. The SI value "0" represents a monodisperse distribution, while the value "1" represents a polydisperse distribution. This analysis could establish that prepared AgNPs showed high monodispersity [48].

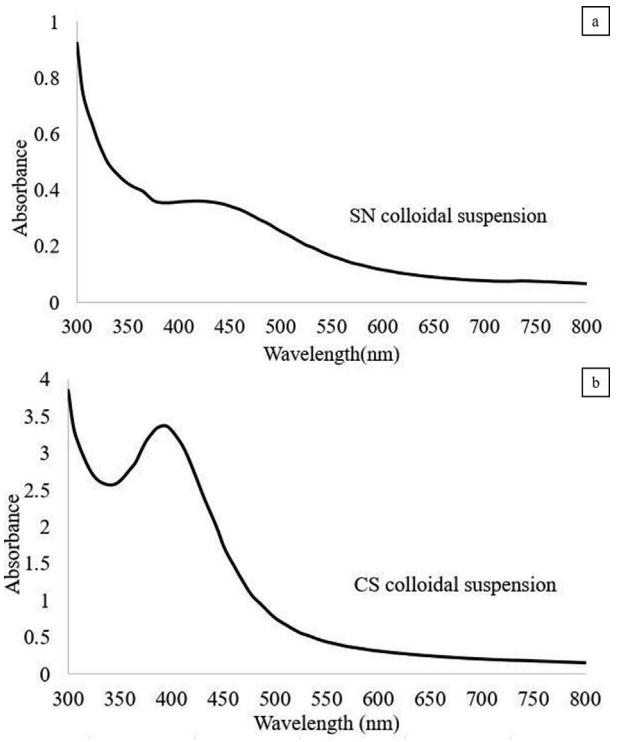


**Figure 1.** UV-Vis spectra for synthesized AgNPs, by using Anamorph R1 Fungus Bjerkandera sp for an incubation temperature of 35 °C and pH 9.0. a. SN colloidal suspension b. CS colloidal suspension.

The synthesis of AgNPs using the fungus Anamorphous Bjerkandera sp. involves the chemical reduction of Ag+ to $Ag^0$ by secondary metabolites including protein tyrosine residues [49]. Within this process of AgNPs formation, in the first instance nucleation occurs, where $Ag^0$ atoms form small silver nuclei; then, a growth phase occurs, where these nuclei start to cluster, and finally a coating is generated, where functional groups associated to these proteins surround the surface of the AgNPs, in this case these substances can control the nucleation and growth of these metallic structures, resulting in the stabilization of the AgNPs [50].

In the mycelium pellet sediment reduction reaction, Ag+ ions are adsorbed on the mycelium surface, due to the electrostatic interaction between Ag+ and the negatively charged functional groups found in this area [51]. Subsequently, the silver ions are reduced by protein residues available in the cell wall; this leads to the formation of silver nuclei, which are released into solution (SN suspension) [49]. Tyrosine, in its chemical structure contains a phenolic –OH group which is the main functional group responsible for the reduction and a –COOH group which can act as a capping agent stopping the growth of silver nuclei during their formation [52]. In this experiment the pH of tyrosine was above its isoelectric point (pI of 5.6) and possibly the –COOH group could have

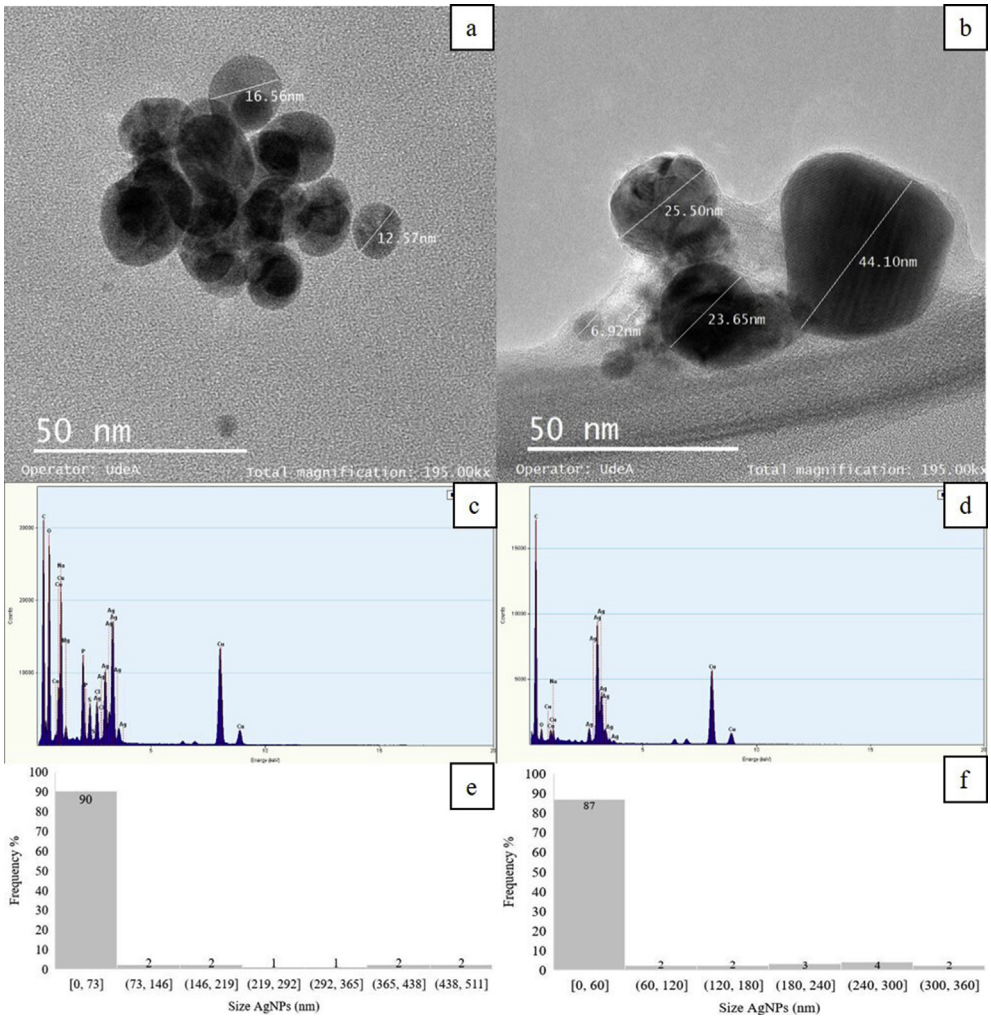


**Figure 2.** Electronic Transmission Microscopy (TEM) images of synthesized silver nanoparticles a) SN colloidal suspension b) CS colloidal suspension. EDS spectrum c) CS sample d) SN sample. Frequency distribution of AgNPs sizes synthesized from the Anamorph R1 Fungus Bjerkandera sp e) CS sample f) SN sample.

changed –COO, and the –OH group to –O, confirming that the anionic form of the amino acid is possibly responsible for the electron transfer to the silver ion in the synthesis process [52, 53, 54, 55] In this case, at the time of the process, the total pH of the reaction was probably increasing (pH > 9), causing the ionization of its phenolic group, transforming the structure into a heterocyclic compound [49, 56].

Under these conditions in the colloidal SN suspension, the mean size of AgNPs could have increased and the concentration of AgNPs could have decreased, due to variations in the nucleation of Ag+ species [50]. In this process, membrane permeability was affected, causing little extracellular substance (protein residues) to accumulate between the mycelial interstices [49]. In this case, fewer nucleation regions may have formed due to the low availability of OH– ions [57, 58], leading to the formation of aggregates (increase the mean size of nanoparticle) through the adsorption of nanocrystals on the mycelial surface.

Compared to the colloidal CS suspension, there were more ***protein*** residues in the fungal extract and it is more likely that more nucleation regions were formed under these conditions due to the availability of OH– ions accelerating the electron transfer to Ag+ ions. In this process, possibly more coating of the silver nuclei was generated, due to a higher presence of COO– groups, facilitating the increase of the nucleation rate and shifting the reaction towards the growth stage (at this stage the nucleation process stops) producing less agglomeration within this solution and a reduction of the mean size of the synthesized AgNPs [52, 57, 58].

These results confirm the findings shown in Figures 1 and 2, where it was determined that the mean size of the synthesized AgNPs within the SN solution increased and the concentration low compared to the CS colloidal suspension.

### *3.2. Characterization of chitosan/carboxymethyl cellulose dressings supplemented with silver nanoparticles*

Figure 3 shows that the manufactured chitosan and carboxymethyl cellulose (CHI-CMC) wound dressings became a bright grayish transparent color. No coloring changes were observed once the various colloidal suspensions of silver nanoparticles (AgNPs) were added. These results yielded structurally adequate wound dressings (Figure 3a–3c) and it was observed that both the CMC concentration (1.2%) and the percentage of glycerol did not affect characteristics of the CHI matrix. To check the above, in the first instance, it could be observed through the optical microscope, in the control sample (Figure 3d), the formation of homogeneous surface structures with a compact structural integrity, by showing, in some portions of the wound dressings, an assembly superimposed in a single direction. With respect to wound dressings containing 1% v/v of the AgNPs suspensions, the formation of heterogeneous surface structures with a semi-compact and porous integrity, where the AgNPs were embedded, with small portions overlapping in different directions (Figure 3e and 3f) were observed for both samples (CS and SN).

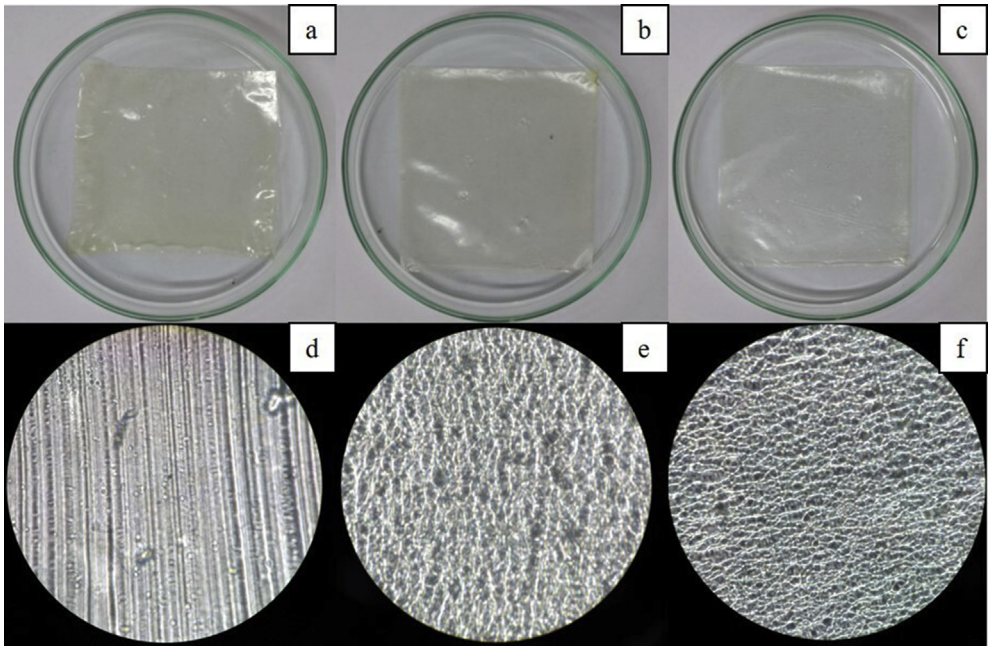


**Figure 3.** CHI-CMC wound dressings a) without the presence of AgNPs; b) with the presence of AgNPs. CS colloidal suspension and c) with presence of AgNPs. SN colloidal suspension. Optical microscope images of CHI-CMC wound dressings 40X (d) without the presence of AgNPs; e) with the presence of AgNPs. CS sample, and f) with presence of AgNPs. SN sample.

Researchers have reported good chemical physical properties of dressings when using CHI-CMC polymer matrices [16, 59]. The afore mentioned results showed that the AgNPs caused changes in the morphology of the wound dressings, by making the surface more porous and rougher (Figure 3e and 3f). This behavior can be a very important indication as to the application of the CHI-CMC-AgNPs wound dressings obtained because first, these morphological characteristics could help to absorb the exuded wounds to be treated and would likely increase the oxygen exchange on the surface of the wound. Thus, showing its versatility for application in healing processes [60].

Images obtained by scanning electron microscopy (SEM) show that CHI-CMC wound dressings has a flat, smooth surface (Figure 4a). Wound dressings containing AgNPs showed a compact and dense structure with accumulation of evenly dispersed nanoparticles on the surface of the films at approximately 60–200 nm (Figure 4b and 4c). These images showed no significant changes with respect to the control sample. The preservation of this smooth structure may have been due in general to two aspects: first, to the structure of CHI, and the ability of CHI to bind and coat the AgNPs aggregates on the film surface; due to the presence of numerous amino groups in CHI, it tends to form coordination bonds with the AgNPs [61]; Secondly, this type of interactions triggers a better compatibility with the CMC structure, stabilizing the compound at the time of preparation. This behavior possibly prevented the formation of roughness on the surface of the film once it was dried [34, 62]. On the other hand, the CHI-CMC-AgNPs wound dressings from the SN colloidal suspension yielded a more homogeneous distribution of AgNPs compared to CHI-CMC-AgNPs wound dressings from CS samples. The reduced mean size of the AgNPs, in this case, found in CS colloidal suspension establishes a larger surface area of the AgNPs and possibly this behavior increased the level of aggregation/agglomeration, which resulted in a less uniform distribution of AgNPs on the surface of the dressing [63, 64]. This result is also consistent with what is reported by Madian and Mohamed [65] and may be a notable indication, in which the non-homogeneity of the distribution of AgNPs can be related to the surface of the polymer matrix with a higher concentration of the latter.

Fouda *et al.*, in their research, described that AgNPs obtained from honey extracts were evenly distributed on the surface of carrageenan biofilms, by forming small island clusters, described that this phenomenon may have been presented because some of these synthesized particles are coated by polysaccharides and proteins. Therefore, a physical barrier was created, which prevented the diffusion of silver through the solution, by forming small agglomerations [66]. In this study, the same effect was reflected (Figure 4b and 4c), and the EDX spectra of synthesized AgNPs in both samples of AgNPs (Figure 2c and 2d) showed that these particles were possibly coated with remnant protein residues in the interstitial spaces of the fungal mycelium [49]. This probably created a physical barrier, which prevented the dissemination of AgNPs once the CHI-CMC wound dressings were prepared.

### 3.3. Mechanical assays

The mechanical properties measured in the tensile test of the chitosan and carboxymethyl cellulose (CHI-CMC) samples, as well as those with silver nanoparticles (CHI-CMC-AgNPs), are an important assessment criterion for wound dressings.

According to the data obtained (Table 1, Figure 5), it was established that AgNPs supplementation increased tensile strength (TS) and elasticity module (EM) of CHI-CMC wound dressings. An increase in the concentration of synthesized AgNPs, e.g., from the SN colloidal suspension, increased TS from 3.27 MPa (control without AgNPs) to 9.77 MPa. With respect to particles synthesized from the CS sample, the same behavior was observed, and there was an increase of 5.14 MPa. These results are consistent with what was reported by Salari *et al.*, Wong and Ramli, suggest that CMC concentration may influence the morphological and mechanical properties of manufactured wound dressings [34, 67]. Another important point, as reported in Table 1, suggests that the mean size of AgNPs played an important role on the mechanical properties of the manufactured dressing. The AgNPs synthesized in the fungal extract (CS colloidal suspension), having a smaller mean size, and thus larger surface area, tend to accumulate more, forming larger aggregates compared to SN colloidal suspension. Under these conditions, possibly the stress-strain transport from the polymers to the nanoparticles and/or aggregates was reduced, causing the mechanical properties of the CHI-CMC-AgNPs-CS dressing decrease with respect to the CHI-CMC-AgNPs-SN dressing [63, 64].

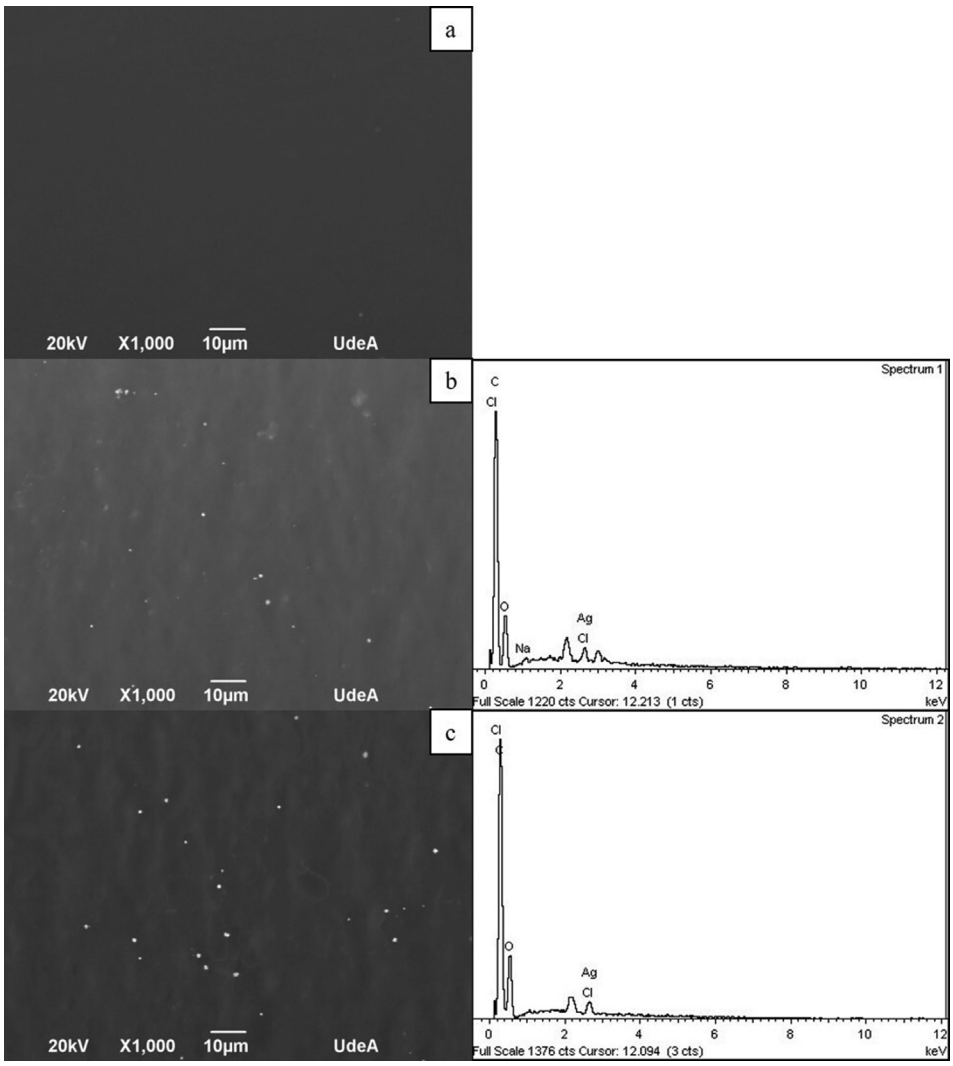


**Figure 4.** SEM micrographs of CHI-CMC wound dressings a) without the presence of AgNPs; b) with the presence of AgNPs. CS mixture, and c) with presence of AgNPs. SN mixture with its respective compositional analysis.

The ANOVA, which is presented in Table 2, did not detect a significant difference p. 0.1487 ($p > 0.05$) between each level evaluated, by suggesting that tensile strength (TS) was not affected by the incorporation of different types of AgNPs suspensions into the polymer matrix. Based on the results specified in Table 1, the increase in TS and elastic module (EM) with respect to the control sample could be attributed to the physical interaction between the polymer matrix and the AgNPs. In this case, the distribution of AgNPs created great interfacial contact with CHI-CMC matrixes, which led to an increase in tensile strength [68, 69]. It is well known that AgNPs and chitosan make up a compact structure due to chemical bonds between electron-rich components such as nitrogen and solitary pairs in silver orbitals [70, 71]. Possibly, this behavior, the homogeneous dispersion of CHI-CMC, and the extremely high surface area of biologically synthesized AgNPs acted as reinforcement elements of CHI-CMC, by creating a stable filler-matrix interface, which considerably improved the mechanical properties of the TS and EM [34, 72].

Regarding the CHI-CMC (control) sample, it could be observed that the tensile strength (TS) and elastic module (EM) were lower relative to the wound dressings, which had AgNPs incorporated. Bao *et al.*, in their

**Table 1.** Thickness, tensile strength (TS), elastic module (EM), and maximum elongation of manufactured wound dressings.

| Sample | Thickness (mm) | Tensile strength (MPa) | Elastic module (MPa) | Maximum elongation (%) |
|---|---|---|---|---|
| CHI-CMC | 0.115 ± 0.007 | 3.27 ± 0.94 | 11.7 ± 0.7 | 25.8 ± 5.7 |
| CHI-CMC-AgNPs-CS | 0.070 ± 0.014 | 5.14 ± 1.54 | 10.4 ± 0.7 | 46.8 ± 4.6 |
| CHI-CMC-AgNPs-SN | 0.055 ± 0.020 | 9.77 ± 3.77 | 13.2 ± 4.9 | 50.8 ± 0.1 |

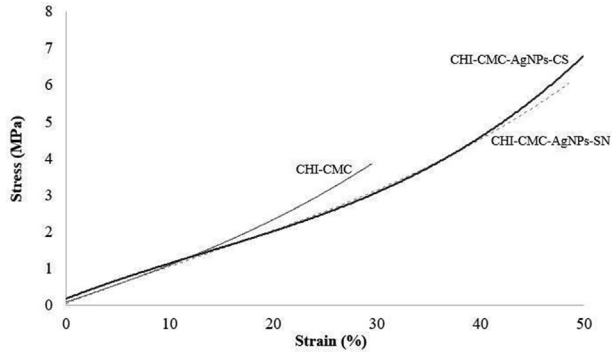


**Figure 5.** Stress-strain graph. Evaluation of the mechanical properties of manufactured wound dressings.

**Table 2.** Variance analysis for the maximum tensile and elongation resistance variables. Mechanical essays of manufactured CS-CMC-AgNPs would dressings.

| Property | Source | Sums of squares | Gl | Mean square | F-Ratio | P-Value |
|---|---|---|---|---|---|---|
| Tensile strength | Between groups | 44.845 | 2 | 22.422 | 3.84 | 0.1487 |
| | Within groups | 17.500 | 3 | 5.833 | | |
| | Total (Corr.) | 62.345 | 5 | | | |
| Maximum elongation | Between groups | 462.666 | 2 | 231.333 | 32.01 | 0.0095 |
| | Within groups | 21.683 | 3 | 7.228 | | |
| | Total (Corr.) | 484.349 | 5 | | | |

research, found good results of tensile strength when there was a cross-link between the two polymers regarding to what was found in this work [17]. It is suggested that in this process, the decrease in TS and EM may have occurred due to the manufacturing method used, the drying time of the wound dressings, the environmental conditions and, in greater proportion, to the concentration of CMC used (1.2 %). Under these conditions, the bonding of the CMC polymer, by considering the drying time of the wound dressings, may have affected the structural integrity of the CS polymer matrix. In this regard, the mixture of both components may have increased the amorphous phase fraction (decrease in crystalline) [59], which weakened the bonding affinity and triggered the decrease in mechanical strength of manufactured wound dressings.

On the other hand, the percentage of elongation of the samples increased, by adding AgNPs, by giving a value of p-0.0095 ($p < 0.05$), and it was observed that for all AgNPs synthesized from both colloidal suspensions, there was an increase of up to 1.7% with respect to control (Table 2). Several authors have proposed that the presence of nanoparticles in the chitosan matrix creates a compact structure, with increased continuities within the polysaccharides network, by leading to a decrease in maximum elongation [28, 73, 74]. Different behavior was observed for these manufactured films, and the effect of AgNPs on increased maximum elongation could be mainly due to the partial substitution of the CHI polymer with the nanoparticles in the film [34]. This behavior along with the reinforcement of the CMC matrix caused a better interconnection of particles with each other in order to make up a compact structure, which reinforced the mechanical properties of the wound dressings (Table 1, Figure 5). The introduction of AgNPs, in this case, improved the crystallinity of the CHI-CMC matrix, by causing a substantial increase in maximum elongation [68]. These results were consistent with what was reported by Salari *et al.* [34]. Besides, the decrease in thickness with respect to the control sample (CHI-CMC), and the good mechanical properties found, suggest that the durability of the manufactured wound dressings could have been improved.

In general, the improvement of the mechanical properties of CHI-CMC-AgNPs films with respect to CHI-CMC could be attributed to different factors such as the homogeneous dispersion of the nanoparticle aggregates and the favorable interactions between the nanoparticles and the polymer matrix. The results showed that possibly the intermolecular bonds between the AgNPs aggregates, the hydroxyl groups (–OH) of the CMC chains and the amino groups (–NH2) of the CHI, resulted in a less rigid and more compact structure, in this case facilitating the effective charge transfer from the polymeric components to the nanoparticles. This type of behavior reflected the good performance of the dressings with respect to tensile strength (TS) and maximum elongation (EM) [34, 62, 65, 75].

Finally, it should be noted that according to Figure 5, manufactured wound dressings have linear viscoelastic behavior. It was found in this experiment, as reported by Ghalei *et al.* that the mechanical properties of the manufactured wound dressings were in the tensile strength ranges close to those reported for human skin, approximately 1–32 MPa [76]. This indicated that this type of wound dressings supplemented with biologically synthesized AgNPs from ligninolytic fungus Anamorphous *Bjerkandera* sp. R1 can be considered sufficiently suitable for applications in wound dressings.

**Table 3.** Average values of the bacterial inhibition experiment performed, by using the bacterium *E. coli.*

| Organism | Initial diameter (mm) | Inhibition zone diameter (mm) | | |
|---|---|---|---|---|
| *Escherichia coli* | | CHI-CMC-AgNPs-CS | CHI-CMC-AgNPs-SN | Control |
| | 12 | 32.9 ± 2.2 | 31,0 ± 4.9 | ND |

### 3.4. Antimicrobial assays

These assays revealed that wound dressings forming solutions (CHI-CMC-AgNPs) inhibited growth, by showing pronounced antimicrobial activity against the pathogen *Escherichia coli (E. coli)* (Table 3). The wound dressings made up of only of biopolymers without the addition of the AgNPs suspensions showed an inhibition zone, but around the 3 halos (Figure 6c) evaluated, formed spores. Thus, it is concluded that there was little or almost no inhibitory activity against the pathogen Gram-negative *E. coli* (Table 3). These results showed that the antimicrobial ineffectiveness of the CHI-CMC forming solutions, was dependent on CMC concentration, and it suggests that antimicrobial activity may exist only due to the CHI matrix. Under these conditions, the antimicrobial effects of CHI decayed markedly because CMC was able to inhibit interactions between the protonic amino groups of CHI and the anionic components of the bacterium *E. coli* [77].

The bactericidal action of AgNPs has been widely studied, and according to various research, can be exerted through different mechanisms [78], but the most accepted main mechanism derives from the ability of the AgNPs complex to induce the generation of reactive oxygen species and oxidative stress [23, 79, 80]. As for the results found and noting that these wound dressings supplemented with AgNPs greatly inhibited the growth of *E. coli* (Figure 6a and 6b), it can be said that the mean size of AgNPs played an important role within the suspension once the wound dressings was prepared. As noted above, due to the mean size obtained from AgNPs 10–50 nm, mainly for the CS sample (Figure 2f), it is easier that these could have spread through the microbial membrane, greatly increasing cell permeability, thus inhibiting the bacterial growth even more.

In this assay, the good antimicrobial activity of the two AgNPs suspensions against this bacterium may have been related, possibly, between the interaction of positively charged silver ions with negatively charged nucleic acids and some bio-macromolecular components (protein residues, which acted as stabilizing and coating agents of AgNPs). These interactions possibly caused structural changes, protein denaturation, and deformation in the cell wall of *E. coli*, by smoothing the cell and causing its death [23, 79, 80, 81, 82].

To validate the results described above, it was intended to demonstrate the effect that the different CHI-CMC-AgNPs solutions have on the growth of the bacteria. Table 4 presents the ANOVA for the halo inhibition response variable. According to the values achieved p. 0.0202 ($p \leq 0.05$) with a confidence level of 95%, it could be established that there was a statistically significant difference between the inhibition halos found between each of the levels evaluated (different CS and SN colloidal suspensions), and it was possible to effectively confirm the AgNPs synthesized in the culture medium further inhibit the growth of the bacteria regarding AgNPs obtained from sediments released by the fungus. These results support what is reported by some researchers, such as Salari *et al.*, Hajji *et al.* and Zheng *et al.* and confirms that since the peptidoglycan

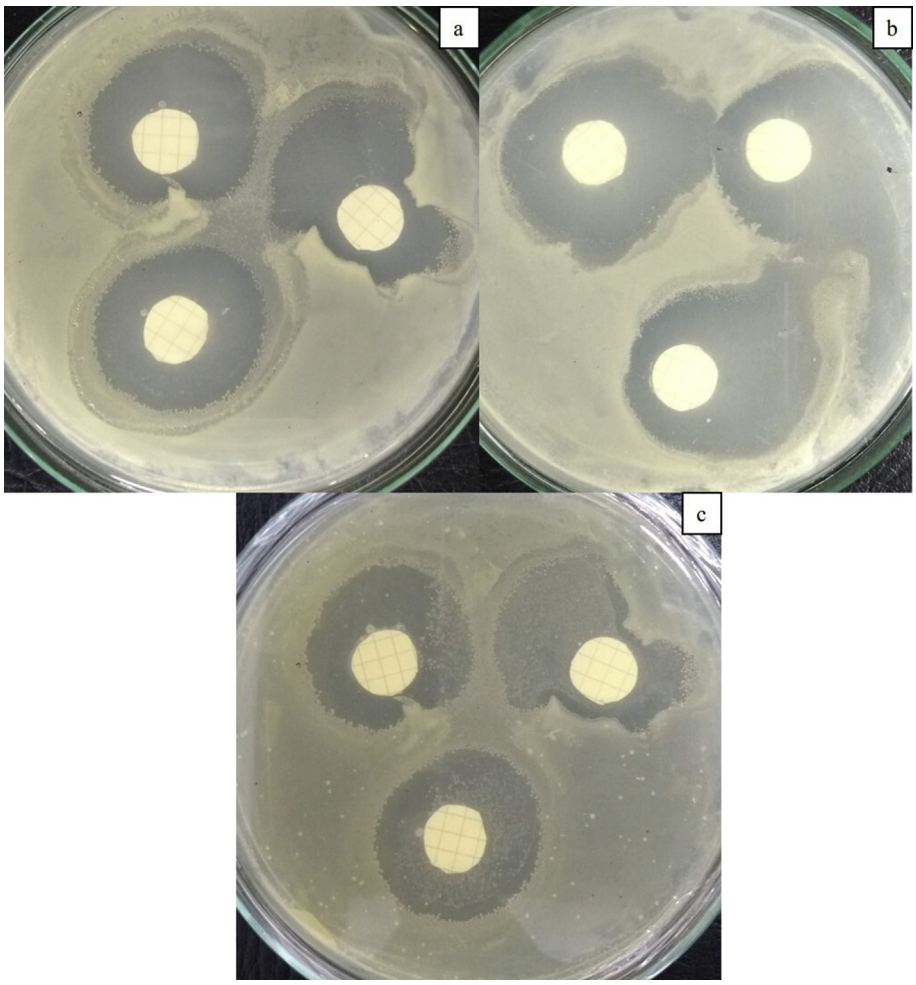


**Figure 6.** Appearance of inhibition zones in nutritious agar plates. The antimicrobial activity of CHI-CMC-AgNPs CS wound dressings is shown, a) SN mixture, b) CS mixture, c) CS-CMC control wound dressings, against Gram-negative bacterium *E. coli.*

(~7–8 nm) cell wall of *E. coli* is so thin, it makes it easier to transport AgNPs into the cell (cytoplasm), and possibly regarding AgNPs of the CS sample, there was better interaction with the surface of the bacteria, specifically, capturing a greater amount of the silver ions [34, 81, 83].

According to the above, it can be suggested that the antimicrobial spectrum of the AgNPs supplemented dressings may be due to the effect of CHI on *E. coli* bacteria. Gram-negative bacteria have a hydrophilic nature and their outer membranes are made up of lipopolysaccharides containing phosphate groups that make the cell surface negatively charged and more sensitive to Chitosan (CHI). Moreover, the antibacterial properties of CHI and AgNPs were not compromised by their chemical structure, providing greater efficacy against this pathogen [61, 84].

### 3.5. Cell viability assays

Detroit cells cultured with wound dressings with different colloidal suspensions of AgNPs (CS and SN colloidal suspensions) of materials at maximum concentration (100%) showed feasibility rates greater than 98%, comparable to what was observed in untreated control cells that had 100% viability. For their part, cells treated with dimethyl sulfoxide (DMSO) 6% showed a clear decrease in their viability (Figure 7). The results were expressed as the percentage of viability of cells cultured with extract of untreated control materials vs cells and cells treated with DMSO 6%. The data corresponds to the average value (X) + the standard deviation of a duplicate test.

Figure 8 shows the images obtained during the cultivation of Detroit cells with extract of materials at maximum concentration, untreated control cells, and cells treated with DMSO 6% (Positive cytotoxicity control). It was observed that cells cultured with CHI-CMC-AgNPs wound

**Table 4.** Variance analysis for the halo inhibition variable. Antimicrobial assay of manufactured CHI-CMC-AgNPs dressings.

| Source | Sum of squares | Gl | Mean square | F-Ratio | P-Value |
|---|---|---|---|---|---|
| Between groups | 118.964 | 3 | 39.655 | 3.95 | 0.02 |
| Within groups | 241.143 | 24 | 10.048 | | |
| Total (Corr.) | 360.107 | 27 | | | |

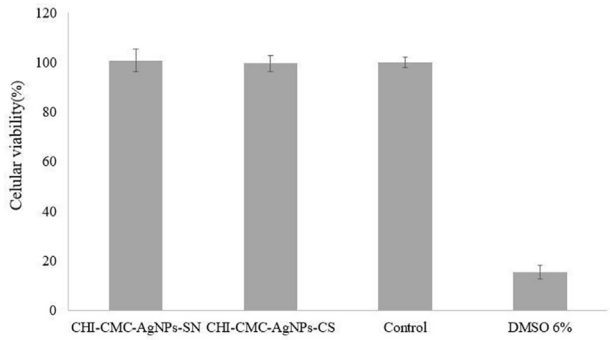


**Figure 7.** Percentages of viability of Detroit cells cultured with material extracts at maximum concentration vs untreated control cells and DMSO-treated cells 6% (positive toxicity control).

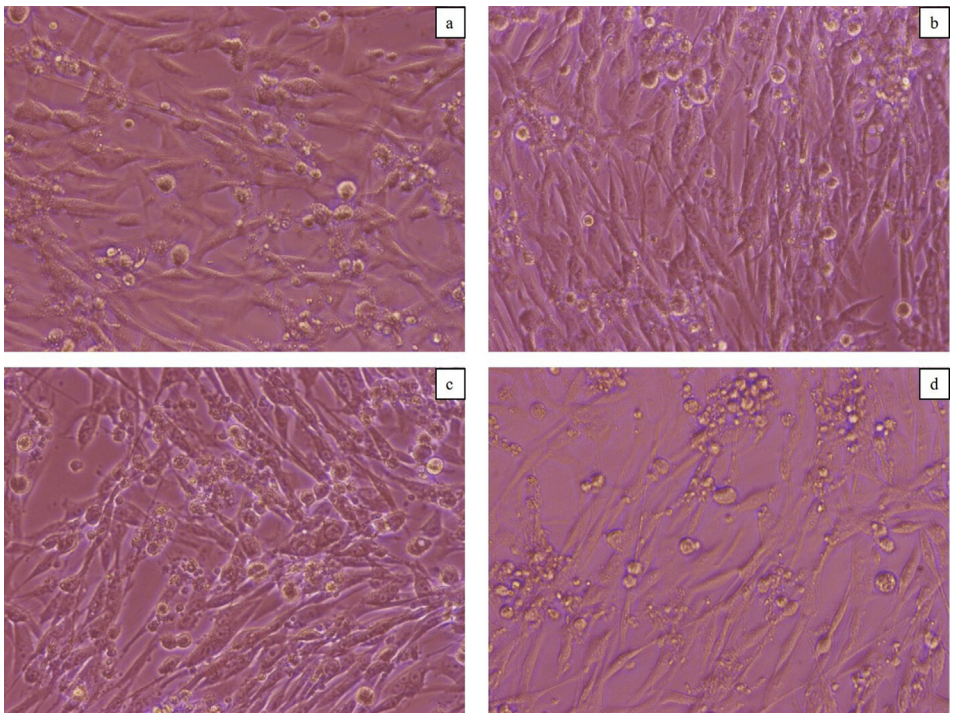


**Figure 8.** Detroit cell culture. a) With CHI-CMC-AgNPs-SN wound dressings, b) With extract with CHI-CMC-AgNPs-CS wound dressings, c) Untreated control cells, and d) 6% DMSO cultured cells (Positive cytotoxicity control). Optical microscopy20 X.

dressings extract and untreated control cells are feasible, with the formation of a monolayer and characteristic morphology. Several parameters with respect to AgNPs, such as size, shape, degree of agglomeration, chemical composition of the surface, load, concentration and exposure time can significantly influence the toxicity of the nanomaterial [85]. Regarding what was found in this research, it is suggested that the low or almost zero cytotoxicity of AgNPs synthesized from the ligninolytic fungus Anamorphous *Bjerkandera* sp. R1 compared to human skin fibroblasts could be thanks to the sizes obtained, morphology, low polydispersity, low agglomeration, and especially, coating agents, such as protein residues (Figure 2a–2d), which are formed within the synthesis process. Thanks to these coatings, biocompatible particles with good antimicrobial properties were obtained, and in the future, they can be considered as a powerful tool in the field of nanomedicine for the manufacture of new wound dressings. In this case, the homogeneous dispersion promoted by the chemical interaction between the polymeric CHI-CMC [86, 87, 88], the surface area, and the protein coatings of these AgNPs acted as an important platform that contribute to improving the antimicrobial spectrum of these dressings without affecting their biocompatibility (cell proliferation). These results are consistent with the work done by Saravanan *et al.*, who reported elevated cellular viability of AgNPs synthesized from the ligninolytic fungus of *Phenerochaete chrysosporium* wood (MTCC787) when evaluated, by using mouse fibroblast cells [25].

## 4. Conclusions

In this work, in the first instance, through conventional microscopy, it was corroborated that biologically synthesized AgNPs caused changes in the morphology of the chitosan-carboxymethyl cellulose wound dressings (CS-CMC-AgNPs), by converting the porous and rough surface. SEM micrographs showed that the AgNPs from the SN colloidal suspension dispersed uniformly across the surface of the dressings, forming fewer agglomerates than the CS colloidal suspension. Agglomerates were observed to have AgNPs in a range of 60–200 nm with quasi-spherical morphology. This indicated that on the surface of the wound dressings the AgNPs was stabilized due to the protein layer with which they were coated.

As for antimicrobial activity against Gram-negative bacterium *E. coli*, the mechanical properties and biocompatibility of CHI-CMC-AgNPs wound dressings, the results showed that wound dressings with the presence of these nanoparticles exhibited strong microbial activity against this pathogen, excellent cellular viability dealing with human skin fibroblasts and good mechanical properties comparable to the reported tensile strength for skin tissue. These findings suggest that such wound dressings treated with AgNPs synthesized from the ligninolytic fungus Anamorphous *Bjerkandera* sp. R1 have a high potential to be applied as a biomaterial in specific areas of biomedicine, such as tissue engineering.

## Declarations

### *Author contribution statement*

Jerónimo Osorio Echavarría: Conceived and designed the experiments; Performed the experiments; Analyzed and interpreted the data; Contributed reagents, materials, analysis tools or data; Wrote the paper.

Natalia Andrea Gómez Vanegas: Conceived and designed the experiments; Performed the experiments; Contributed reagents, materials, analysis tools or data.

Claudia Patricia Ossa Orozco: Conceived and designed the experiments; Performed the experiments; Analyzed and interpreted the data; Contributed reagents, materials, analysis tools or data.

### *Funding statement*

This research did not receive any specific grant from funding agencies in the public, commercial, or not-for-profit sectors.

### *Data availability statement*

Data included in article/supplementary material/referenced in article.

## Declaration of interests statement

The authors declare no conflict of interest.

## Additional information

No additional information is available for this paper.

## References


[1] A.R. Fajardo, L.C. Lopes, A.O. Caleare, E.a. Britta, C.V. Nakamura, A.F. Rubira, E.C. Muniz, Silver sulfadiazine loaded chitosan/chondroitin sulfate films for a potential wound dressing application, Mater. Sci. Eng. C 33 (2013) 588–595.

[2] J.E. Lai-Cheong, J.a. McGrath, Structure and function of skin, hair and nails, Medicine (United Kingdom). 45 (2017) 347–351.

[3] D. Simões, S.P. Miguel, M.P. Ribeiro, P. Coutinho, A.G. Mendonça, I.J. Correia, Recent advances on antimicrobial wound dressing: a review, Eur. J. Pharm. Biopharm. 127 (2018) 130–141.

[4] A. Moeini, P. Pedram, P. Makvandi, M. Malinconico, G. Gomez, Wound healing and antimicrobial effect of active secondary metabolites in chitosan-based wound dressings: a review, Carbohydr. Polym. 233 (2020) 1–15.

[5] S. Asghari, S. Logsetty, S. Liu, Imparting commercial antimicrobial dressings with low-adherence to burn wounds, Burns 42 (2016) 877–883.

[6] J. Wang, M. Windbergs, Functional electrospun fibers for the treatment of human skin wounds, Eur. J. Pharm. Biopharm. 119 (2017) 283–299.

[7] J.L. Velázquez-Velázquez, A. Santos-Flores, J. Araujo-Meléndez, R. Sánchez-Sánchez, C. Velasquillo, C. González, G. Martínez-Castañon, F. Martinez-Gutierrez, Anti-biofilm and cytotoxicity activity of impregnated dressings with silver nanoparticles, Mater. Sci. Eng. C. Mater. Biol. Appl. 49 (2015) 604–611.

[8] a. Sathiyaseelan, A. Shajahan, P.T. Kalaichelvan, V. Kaviyarasan, Fungal chitosan based nanocomposites sponges-An alternative medicine for wound dressing, Int. J. Biol. Macromol. 104 (2016) 1905–1915.

[9] S. Azizi, R. Mohamad, R. Abdul Rahim, R. Mohammadinejad, A. Bin Ariff, Hydrogel beads bio-nanocomposite based on Kappa-Carrageenan and green synthesized silver nanoparticles for biomedical applications, Int. J. Biol. Macromol. 104 (2017) 423–431.

[10] G.D. Mogoşanu, A.M. Grumezescu, Natural and synthetic polymers for wounds and burns dressing, Int. J. Pharm. 463 (2014) 127–136.

[11] H. Hamedi, S. Moradi, S.M. Hudson, A.E. Tonelli, Chitosan based hydrogels and their applications for drug delivery in wound dressings: a review, Carbohydr. Polym. 199 (2018) 445–460.

[12] M. Naseri-Nosar, Z.M. Ziora, Wound dressings from naturally-occurring polymers: a review on homopolysaccharide-based composites, Carbohydr. Polym. 189 (2018) 379–398.

[13] E.a. Kamoun, E.R.S. Kenawy, X. Chen, A review on polymeric hydrogel membranes for wound dressing applications: PVA-based hydrogel dressings, J. Adv. Res. 8 (2017) 217–233.

[14] S. Bin Park, E. Lih, K.S. Park, Y.K. Joung, D.K. Han, Biopolymer-based functional composites for medical applications, Prog. Polym. Sci. 68 (2017) 77–105.

[15] N. Masood, R. Ahmed, M. Tariq, Z. Ahmed, Silver nanoparticle impregnated chitosan-PEG hydrogel enhances wound healing in diabetes induced rabbits, Int. J. Pharm. 559 (2019) 23–36.

[16] D. Hu, T. Qiang, L. Wang, Quaternized chitosan/polyvinyl alcohol/sodium carboxymethylcellulose blend film for potential wound dressing application, Wound Med 16 (2017) 15–21.

[17] D. Bao, M. Chen, H. Wang, J. Wang, C. Liu, R. Sun, Preparation and characterization of double crosslinked hydrogel films from carboxymethylchitosan and carboxymethylcellulose, Carbohydr. Polym. 110 (2014) 113–120.

[18] L. Vinklárková, R. Masteiková, G. Foltýnová, J. Muselík, S. Pavloková, J. Bernatonienė, D. Vetchý, Film wound dressing with local anesthetic based on insoluble carboxymethycellulose matrix, J. Appl. Biomed. 15 (2017) 313–320.

[19] M.I.N. Ahamed, S. Sankar, P.M. Kashif, S.K.H. Basha, T.P. Sastry, Evaluation of biomaterial containing regenerated cellulose and chitosan incorporated with silver nanoparticles, Int. J. Biol. Macromol. 72 (2015) 680–686.

[20] S.S.D. Kumar, N.K. Rajendran, N.N. Houreld, H. Abrahamse, Recent advances on silver nanoparticle and biopolymer based biomaterials for wound healing applications, Int. J. Biol. Macromol. 115 (2018) 165–175.

[21] J. Boateng, O. Catanzano, Advanced therapeutic dressings for effective wound healing - a review, J. Pharmacol. Sci. 104 (2015) 3653–3680.

[22] H.J. Johnston, G. Hutchison, F.M. Christensen, S. Peters, S. Hankin, V. Stone, A review of the in vivo and in vitro toxicity of silver and gold particulates: particle attributes and biological mechanisms responsible for the observed toxicity, Crit. Rev. Toxicol. 40 (2010) 328–346.

[23] P. Rauwel, E. Rauwel, S. Ferdov, M.P. Singh, Silver nanoparticles: synthesis, properties, and applications, Adv. Mater. Sci. Eng. 20 (2015).

[24] G. Krishna, P. Vadapally, M.a. Singara Charya, Biogenic synthesis of silver nanoparticles from white Rot Fungi: their characterization and antibacterial studies, OpenNano (2017).

[25] M. Saravanan, S. Arokiyaraj, T. Lakshmi, A. Pugazhendhi, Synthesis of silver nanoparticles from Phenerochaete chrysosporium (MTCC-787) and their antibacterial activity against human pathogenic bacteria, Microb. Pathog. 117 (2018) 68–72.

[26] A. Hebeish, M. El-Rafie, M. El-Sheikh, A. Seleem, M. El-Naggar, Antimicrobial wound dressing and anti-inflammatory efficacy of silver nanoparticles, Int. J. Biol. Macromol. 65 (2014) 509–515.

[27] G. Juncu, A. Stoica-Guzun, M. Stroescu, G. Isopencu, S.I. Jinga, Drug release kinetics from carboxymethylcellulose-bacterial cellulose composite films, Int. J. Pharm. 510 (2016) 485–492.

[28] D. Archana, B.K. Singh, J. Dutta, P.K. Dutta, Chitosan-PVP-nano silver oxide wound dressing: in vitro and in vivo evaluation, Int. J. Biol. Macromol. 73 (2015) 49–57.

[29] R. Taboada-Puig, T. Lú-Chau, M.T. Moreira, G. Feijoo, M.J. Martínez, J.M. Lema, A new strain of Bjerkandera sp. production, purification and characterization of versatile peroxidase, World J. Microbiol. Biotechnol. 27 (2011) 115–122.

[30] J. Osorio, Evaluación De La Decoloración De Efluentes Industriales En Un Reactor De Lecho Fijo Empleando El Hongo De La Pudrición Blanca De La Madera Anthracophyllum Discolor, Universidad de Antioquia, 2010.

[31] J. Osorio-echavarría, N.A. Gómez-vanegas, J. Osorio-echavarría, C.P. Ossa-orozco, Preparation of carrageenan biofilms mixed with silver nanoparticles by biological synthesis method·Obtención de biopelículas de carragenina suplementadas con nanopartículas de plata sintetizadas biológicamente, Dyna 84 (2017) 82–87.

[32] M.I. Gaviria-Arroyave, J. Osorio-Echavarría, N.A. Gómez-Vanegas, Evaluating the scale-up of a reactor for the treatment of textile effluents using Bjerkandera sp, Rev. Fac. Ing. Univ. Antioquia. 88 (2018) 80–90.

[33] J. Osorio-Echavarría, Mejoramiento de la Síntesis de Nanopartículas de Plata a partir del Hongo Ligninolítico Anamorfo R1 de Bjerkandera sp. y su Evaluación para Aplicación en Apósitos, Universidad de Antioquia, 2020.

[34] M. Salari, M. Sowti Khiabani, R. Rezaei Mokarram, B. Ghanbarzadeh, H. Samadi Kafil, Development and evaluation of chitosan based active nanocomposite films containing bacterial cellulose nanocrystals and silver nanoparticles, Food Hydrocolloids 84 (2018) 414–423.

[35] L. Biao, S. Tan, Y. Wang, X. Guo, Y. Fu, F. Xu, Y. Zu, Z. Liu, Synthesis, characterization and antibacterial study on the chitosan-functionalized Ag nanoparticles, Mater. Sci. Eng. C 76 (2017) 73–80.

[36] V. Sarsar, M.K. Selwal, K.K. Selwal, Biofabrication, characterization and antibacterial efficacy of extracellular silver nanoparticles using novel fungal strain of Penicillium atramentosum KM, J. Saudi Chem. Soc. 19 (2015) 682–688.

[37] B.K. Nayak, A. Nanda, V. Prabhakar, Biogenic synthesis of silver nanoparticle from wasp nest soil fungus, Penicillium italicum and its analysis against multi drug resistance pathogens, Biocatal. Agric. Biotechnol. 16 (2018) 412–418.

[38] S.M. Husseiny, T.A. Salah, H.A. Anter, Biosynthesis of size controlled silver nanoparticles by Fusarium oxysporum, their antibacterial and antitumor activities, Beni-Suef Univ. J. Basic Appl. Sci. 4 (2015) 225–231.

[39] L. De Sio, Active Plasmonic Nanomaterials, first ed., Jenny Stanford Publishing, National Capital Territory (NCT) of Delhi, 2015.

[40] Y. Delgado-Beleño, C.E. Martinez-Nuñez, M. Cortez-Valadez, N.S. Flores-López, M. Flores-Acosta, Optical properties of silver, silver sulfide and silver selenide nanoparticles and antibacterial applications, Mater. Res. Bull. 99 (2018) 385–392.

[41] M. Sikder, J.R. Lead, G.T. Chandler, M. Baalousha, A rapid approach for measuring silver nanoparticle concentration and dissolution in seawater by UV–Vis, Sci. Total Environ. 618 (2018) 597–607.

[42] D. Paramelle, A. Sadovoy, S. Gorelik, P. Free, J. Hobley, D.G. Fernig, Rapid method to estimate the concentration of citrate capped silver nanoparticles from UV-visible light spectra, Analyst 139 (2012) 4855–4861.

[43] S.I. Rasmagin, L.A. Apresyan, Analysis of the optical properties of silver nanoparticles, Opt. Spectrosc. 128 (2020) 327–330.

[44] S.S. Birla, S.C. Gaikwad, A.K. Gade, M.K. Rai, Rapid synthesis of silver nanoparticles from Fusarium oxysporum by optimizing physicocultural conditions, Sci. World J. 2013 (2013) 1–12.

[45] K.B. Mogensen, K. Kneipp, Size-dependent shifts of plasmon resonance in silver nanoparticle films using controlled dissolution: monitoring the onset of surface screening effects, J. Phys. Chem. C 118 (2014) 28075–28083.

[46] P.K. Seetharaman, R. Chandrasekaran, S. Gnanasekar, G. Chandrakasan, M. Gupta, D.B. Manikandan, S. Sivaperumal, Antimicrobial and larvicidal activity of eco-friendly silver nanoparticles synthesized from endophytic fungi Phomopsis liquidambaris, Biocatal. Agric. Biotechnol. 16 (2018) 22–30.

[47] A. Syed, S. Saraswati, G.C. Kundu, A. Ahmad, Biological synthesis of silver nanoparticles using the fungus Humicola sp. and evaluation of their cytoxicity using normal and cancer cell lines, Spectrochim. Acta Part A Mol. Biomol. Spectrosc. 114 (2013) 144–147.

[48] S. Raj, S.C. Mali, R. Trivedi, Green synthesis and characterization of silver nanoparticles using Enicostemma axillare (Lam.) leaf extract, Biochem. Biophys. Res. Commun. 503 (2018) 2814–2819.

[49] J. Osorio-Echavarría, J.O. Osorio-Echavarría, C.P. Ossa-Orozco, N.A. Gómez-Vanegas, Synthesis of silver nanoparticles using white - rot fungus Anamorphous Bjerkandera sp. R1: influence of silver nitrate concentration and fungus growth time, Sci. Rep. 11 (2021) 1–14.

[50] K.M. Soto, C.T. Quezada-Cervantes, M. Hernández-Iturriaga, G. Luna-Bárcenas, R. Vazquez-Duhalt, S. Mendoza, Fruit peels waste for the green synthesis of silver nanoparticles with antimicrobial activity against foodborne pathogens, LWT 103 (2019) 293–300.

[51] Y.S. Chan, M.M. Don, Biosynthesis and structural characterization of Ag nanoparticles from white rot fungi, Mater. Sci. Eng. C 33 (2013) 282–288.

[52] S.B. Maddinedi, B.K. Mandal, K.K. Anna, Tyrosine assisted size controlled synthesis of silver nanoparticles and their catalytic, in-vitro cytotoxicity evaluation, Environ. Toxicol. Pharmacol. 51 (2017) 23–29.

[53] Z. Zaheer, Rafiuddin, Silver nanoparticles formation using tyrosine in presence cetyltrimethylammonium bromide, Colloids Surf. B Biointerfaces 89 (2012) 211–215.

[54] D.I. Saragih, D.C.V. Arifin, B. Rusdiarso, S. Suyanta, S.J. Santosa, Synthesis of silver nanoparticles using tyrosine as reductor and capping agent, Key Eng. Mater. 840 KEM (2020) 360–367.
[55] D.C. Varin Arifin, Antibacterial activity of silver nanoparticles synthesized using tyrosine as capping and reducing agent, Int. J. Emerg. Trends Eng. Res. 8 (2020) 2414–2421.
[56] P.R. Selvakannan, A. Swami, D. Srisathiyanarayanan, P.S. Shirude, R. Pasricha, A.B. Mandale, M. Sastry, Synthesis of aqueous Au core-Ag shell nanoparticles using tyrosine as a pH-dependent reducing agent and assembling phase-transferred silver nanoparticles at the air-water interface, Langmuir 20 (2004) 7825–7836.
[57] S.K. Mehta, S. Chaudhary, M. Gradzielski, Time dependence of nucleation and growth of silver nanoparticles generated by sugar reduction in micellar media, J. Colloid Interface Sci. 343 (2010) 447–453.
[58] M.F. Zayed, W.H. Eisa, S.M. El-kousy, W.K. Mleha, N. Kamal, Ficus retusa-stabilized gold and silver nanoparticles: controlled synthesis, spectroscopic characterization, and sensing properties, Spectrochim. Acta Part A Mol. Biomol. Spectrosc. 214 (2019) 496–512.
[59] J. Kingkaew, S. Kirdponpattara, N. Sanchavanakit, P. Pavasant, M. Phisalaphong, Effect of molecular weight of chitosan on antimicrobial properties and tissue compatibility of chitosan-impregnated bacterial cellulose films, Biotechnol. Bioproc. Eng. 19 (2014) 534–544.
[60] P. Marie Arockianathan, S. Sekar, B. Kumaran, T.P. Sastry, Preparation, characterization and evaluation of biocomposite films containing chitosan and sago starch impregnated with silver nanoparticles, Int. J. Biol. Macromol. 50 (2012) 939–946.
[61] P. Kanniah, P. Chelliah, J.R. Thangapandi, G. Gnanadhas, V. Mahendran, M. Robert, Green synthesis of antibacterial and cytotoxic silver nanoparticles by Piper nigrum seed extract and development of antibacterial silver based chitosan nanocomposite, Int. J. Biol. Macromol. 189 (2021) 18–33.
[62] A.B. Perumal, P.S. Sellamuthu, R.B. Nambiar, E.R. Sadiku, Development of polyvinyl alcohol/chitosan bio-nanocomposite films reinforced with cellulose nanocrystals isolated from rice straw, Appl. Surf. Sci. 449 (2018) 591–602.
[63] Y. Zare, Study of nanoparticles aggregation/agglomeration in polymer particulate nanocomposites by mechanical properties, Compos. Part A. 84 (2016) 158–164.
[64] M.A. Ashraf, W. Peng, Y. Zare, K.Y. Rhee, Effects of size and aggregation/agglomeration of nanoparticles on the interfacial/interphase properties and tensile strength of polymer nanocomposites, Nanoscale Res. Lett. 13 (2018) 1–7.
[65] N. Mohamed, N.G. Madian, Evaluation of the mechanical, physical and antimicrobial properties of chitosan thin films doped with greenly synthesized silver nanoparticles, Mater. Today Commun. 25 (2020) 1–9.
[66] M.M.G. Fouda, M.R. El-Aassar, G.F. El Fawal, E.E. Hafez, S.H.D. Masry, A. Abdel-Megeed, k-Carrageenan/poly vinyl pyrollidone/polyethylene glycol/silver nanoparticles film for biomedical application, Int. J. Biol. Macromol. 74 (2015) 179–184.
[67] T.W. Wong, N.A. Ramli, Carboxymethylcellulose film for bacterial wound infection control and healing, Carbohydr. Polym. 112 (2014) 367–375.
[68] M. Salman, M. Bilal, K. Niazi, Z. Jahan, T. Ahmad, A. Hussain, Preparation and characterization of PVA/nanocellulose/Ag nanocomposite films for antimicrobial food packaging, Carbohydr. Polym. 184 (2018) 453–464.
[69] W. Wang, Z. Yu, F.K. Alsammarraie, F. Kong, M. Lin, A. Mustapha, Properties and antimicrobial activity of polyvinyl alcohol-modified bacterial nanocellulose packaging films incorporated with silver nanoparticles, Food Hydrocolloids 100 (2020) 1–10.
[70] Y. Qin, Y. Liu, L. Yuan, H. Yong, J. Liu, Preparation and characterization of antioxidant, antimicrobial and pH- sensitive films based on chitosan, silver nanoparticles and purple corn extract, Food Hydrocolloids 96 (2019) 102–111.
[71] M. Zienkiewicz-strzałka, A. Deryło-marczewska, Y.A. Skorik, Silver nanoparticles on chitosan/silica nanofibers: characterization and antibacterial activity, Int. J. Mol. Sci. 21 (1) (2019) 1–20.
[72] S.V. Capanema, A.A.P. Mansur, S.M. Carvalho, L.L. Mansur, C.P. Ramos, A.P. Lage, H.S. Mansur, Physicochemical properties and antimicrobial activity of biocompatible carboxymethylcellulose-silver nanoparticle hybrids for wound dressing and epidermal repair, J. Appl. Polym. Sci. 135 (6) (2017) 1–18.
[73] J.W. Rhim, S. Bin Lee, S.I. Hong, Preparation and characterization of Agar/Clay nanocomposite films: the effect of clay type, J. Food Sci. 76 (2011) 40–48.
[74] Y. Xie, X. Liao, J. Zhang, F. Yang, Z. Fan, Novel chitosan hydrogels reinforced by silver nanoparticles with ultrahigh mechanical and high antibacterial properties for accelerating wound healing, Int. J. Biol. Macromol. 119 (2018) 402–412.
[75] S.M.K. Thiagamani, N. Rajini, S. Siengchin, A. Varada Rajulu, N. Hariram, N. Ayrilmis, Influence of silver nanoparticles on the mechanical, thermal and antimicrobial properties of cellulose-based hybrid nanocomposites, Compos. B Eng. 165 (2019) 516–525.
[76] S. Ghalei, J. Nourmohammadi, A. Solouk, H. Mirzadeh, Enhanced cellular response elicited by addition of amniotic fluid to alginate hydrogel-electrospun silk fibroin fibers for potential wound dressing application, Colloids Surf. B Biointerfaces 172 (2018) 82–89.
[77] O.M. Dragostin, S.K. Samal, M. Dash, F. Lupascu, A. Pânzariu, C. Tuchilus, N. Ghetu, M. Danciu, P. Dubruel, D. Pieptu, C. Vasile, R. Tatia, L. Profire, New antimicrobial chitosan derivatives for wound dressing applications, Carbohydr. Polym. 141 (2016) 28–40.
[78] H. Choudhury, M. Pandey, Y. Qing, C. Yee, C. Teck, T. Cheng, L. Marilyn, H. Seang, Y. Ping, C. Feng, Bhattamishra, Silver nanoparticles: Advanced and promising technology in diabetic wound therapy, Mater. Sci. Eng. C 112 (2020) 1–16.
[79] J. Du, Z. Hu, W. Dong, Y. Wang, S. Wu, Y. Bai, Biosynthesis of large-sized silver nanoparticles using Angelica keiskei extract and its antibacterial activity and mechanisms investigation, Microchem. J. 147 (2019) 333–338.
[80] S.M. Navarro, E. Alpaslan, M. Wang, P. Larese-casanova, M.E. Londoño, L. Atehortúa, J.J. Pavón, T.J. Webster, Characterization and study of the antibacterial mechanisms of silver nanoparticles prepared with microalgal exopolysaccharides, Mater. Sci. Eng. C 99 (2019) 685–695.
[81] S. Raja, V. Ramesh, V. Thivaharan, Green biosynthesis of silver nanoparticles using Calliandra haematocephala leaf extract, their antibacterial activity and hydrogen peroxide sensing capability, Arab. J. Chem. 10 (2017) 253–261.
[82] S. Hajji, R.B.S. Ben Salem, M. Hamdi, K. Jellouli, W. Ayadi, M. Nasri, S. Boufi, Nanocomposite films based on chitosan–poly(vinyl alcohol) and silver nanoparticles with high antibacterial and antioxidant activities, Process Saf. Environ. Protect. 111 (2017) 112–121.
[83] S. Lin, L. Chen, L. Huang, S. Cao, X. Luo, K. Liu, Novel antimicrobial chitosan-cellulose composite films bioconjugated with silver nanoparticles, Ind. Crop. Prod. 70 (2015) 395–403.
[84] W.R. Rolim, M.T. Pelegrino, B. De Araújo, L.S. Ferraz, F.N. Costa, J.S. Bernardes, T. Rodigues, M. Brocchi, Green tea extract mediated biogenic synthesis of silver nanoparticles: characterization, cytotoxicity evaluation and antibacterial activity, Appl. Surf. Sci. 463 (2019) 66–74.
[85] H. Abou-Yousef, S. Dacrory, M. Hasanin, E. Saber, S. Kamel, Biocompatible hydrogel based on aldehyde-functionalized cellulose and chitosan for potential control drug release, Sustain. Chem. Pharm. 21 (2021).
[86] D.Z. Zmejkoski, N.M. Zdravković, D.D. Trišić, M.D. Budimir, Z.M. Marković, N.O. Kozyrovska, B.M. Todorović Marković, Chronic wound dressings – pathogenic bacteria anti-biofilm treatment with bacterial cellulose-chitosan polymer or bacterial cellulose-chitosan dots composite hydrogels, Int. J. Biol. Macromol. 191 (2021) 315–323.
[87] S. Wichai, P. Chuysinuan, S. Chaiarwut, P. Ekabutr, P. Supaphol, Development of bacterial cellulose/alginate/chitosan composites incorporating copper (II) sulfate as an antibacterial wound dressing, J. Drug Deliv. Sci. Technol. 51 (2019) 662–671.
[88] T. Gebregiorgis, M. Vaccari, S. Prasad, E.D. Van Hullebusch, S. Rtimi, Preparation and applications of chitosan and cellulose composite materials, J.Environ. Manag. 301 (2022) 1–18.